

AMS modeling of controlled switch for design optimization of capacitive vibration energy harvester

Dimitri Galayko, Rodrigo Pizarro
LIP6
dimitri.galayko@lip6.fr

Philippe Basset, Ayyaz Mahmood Paracha,
Gilles Amendola
ESYCOM-ESIEE
p.basset@esiee.fr

Abstract

This paper presents an analysis, behavioral modeling and functional design of a capacitive vibration energy harvester, composed from a mechanical resonator, capacitive transducer and a conditioning circuit based on the BUCK DC-DC converter architecture. The goal of the study is to identify the optimal scenario of the BUCK switch commutation and to propose a functional model of the switch device. The study included an analysis, design and modeling phases. We found that the optimal commutation timing is defined by the energetical state of the circuit (voltages and currents) rather by a "hard" time specification. The developed VHDL-AMS functional model of the switch was validated by a ADvanceMS multi-physics simulation of the whole harvester. The resonator and capacitive transducer were modeled in VHDL-AMS, the electric elements of the conditioning circuit by their ELDO models.

1 Introduction

With evolution of microelectronic technologies, the miniaturization and integration of electronic systems will be pursued. The microelectronic industry is moving toward very compact, autonomous and pervasive systems which use multi-physics signal processing (like embedded sensors and sensor networks). However, the energy autonomy of such systems remains the key problem, and one of the solutions can be provided by harvesting the energy from the environment. For example, the mechanical (vibrational) energy is omnipresent, especially in the case of transport applications.

A mechanical energy harvester is made from a mechanical resonator, an electromechanical transducer and a conditioning circuit achieving the energy transfer from the transducer toward the electrical load. In this paper, we deal with a capacitive (electrostatic) transducer [1].

The architecture of the conditioning circuit has been an object of numerous studies. It is generally built from a charge pump and a flyback circuit (fig. 1). Although the former has been well studied and its design does not present any major difficulty [2], the latter continues to be

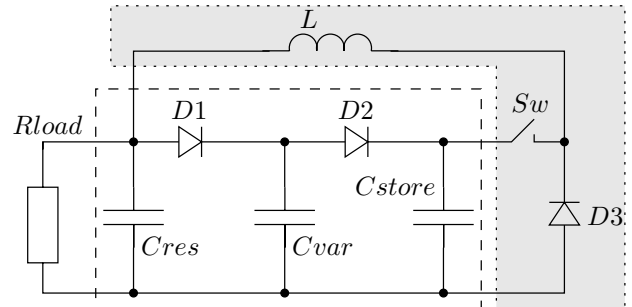


Figure 1: Conditioning circuit of energy harvester inspired from the BUCK DC-DC converter. In dashed frame, the charge pump, in gray, the flyback circuit.

a subject of intensive work. The fig. 1 presents a circuit with a flyback circuit inspired from the BUCK DC-DC converter.

The circuit operation is composed of two phases : energy accumulation (charge pump) and recharge of the buffer capacitor C_{res} (flyback). A commutation between these phases is achieved by the switch Sw which is the main bottleneck of the energy harvester circuit, and is the object of our study. Both its physical realization and choice of functional behavior rise many questions. The goal of our study is to find an optimal operation mode of the switch and to define a functional VHDL-AMS model describing it, making an abstraction on the realization issues. As we will see, this approach offers a great freedom for the design solution exploration. This description can be used as specifications for a physical switch realization.

A reliable modeling of the whole system is a key point for the successful design, since an energy harvester is a nonlinear multivariate system with a strong coupling between the mechanic and electric phenomena. The resonator and the electromechanical transducer are naturally represented by behavioral models based on their physical equations. The electrical part is usually modeled using electrical SPICE-like simulators. In this paper we present a complete VHDL-AMS mixed with ELDO model of the whole system "resonator-transducer-conditioning circuit" and show its use for an extended study of the circuit.

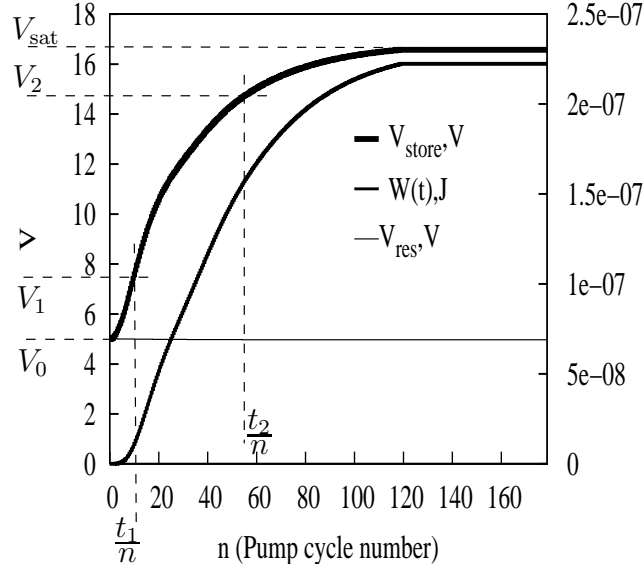


Figure 2: Pump charge operation : V_{store} , V_{res} and gained energy curves.

2 Harvester operation

2.1 Charge pump

The charge pump operates when the switch Sw is off.

Let the initial condition of the charge pump are as follows : $V_{res} = V_{store} = V_{var} = V_0$, $C_{var} = C_{max}$. When the resonator vibration makes C_{var} to decrease, V_{var} increases, $D1$ is off and $D2$ is on: charges from C_{var} flues on C_{store} . Once reaching its minimum, C_{var} starts to increase and $D2$ becomes off while V_{var} decreases. When V_{var} reaches the level of V_{res} , $D1$ becomes on and the charges of C_{res} flues toward C_{var} . Iterations of C_{var} variations get V_{var} increase and V_{res} decrease, keeping the total amount of charges constant. Since $C_{var} < C_{res}$, taking a charge ΔQ from C_{store} needs less of energy than putting ΔQ on C_{res} : this energy lack is provided by the C_{var} variations, and actually stored in the system $C_{var} C_{res}$. Fig. 2 presents the evolution of V_{var} and of the harvested energy with the number of iterations.

In practice, $C_{res} \gg C_{store} \gg C_{var}$, and V_{res} remains nearly constant during the operation of the conditioning circuit (fig. 2).

2.2 The flyback operation

The pump charge ends by being saturated when the variations of V_{var} can't switch the diodes on. To continue the energy harvesting, the difference between V_{res} and V_{store} should be reduced (C_{store} should discharge on C_{res}), and the gained energy should be used for the load supply. This is achieved by the flyback circuit. After the action of the flyback circuit, V_{store} reduces from V_2 to some V_1 ($0 < V_1 < V_2$), from which starts the next phase of the charge pumping (fig. 3).

Let the initial conditions for the flyback circuit be the following (at $t = t_2$, fig. 3): the switch is on, $V_{store} - V_{res} = \Delta V_2$, $I_L = 0$. C_{var} is in parallel with C_{res} or C_{store} , depending on the state of $D1$ and $D2$ which is defined by the voltage on C_{var} . However, since C_{var} is small, its contribution to the flyback network operation is neglectable. The resulting LC network (where $C = C_{store}C_{res}/(C_{store} + C_{res})$ and with initial voltage ΔV_2) starts to oscillate: I_L increases and ΔV decreases. The switch has to be closed before $I_L = 0$, i.e., before $T/4$, where $1/T$ is the natural frequency of the LC network. During this transient process, the inductor accumulates the energy gained by the pump, and the capacitor voltages V_{res} and V_{store} evolve toward their initial values. When $V_{res} = V_{store}$, obviously $V_{res} = V_{store} = V_0$ and the inductor contains all the energy gained by the pump.

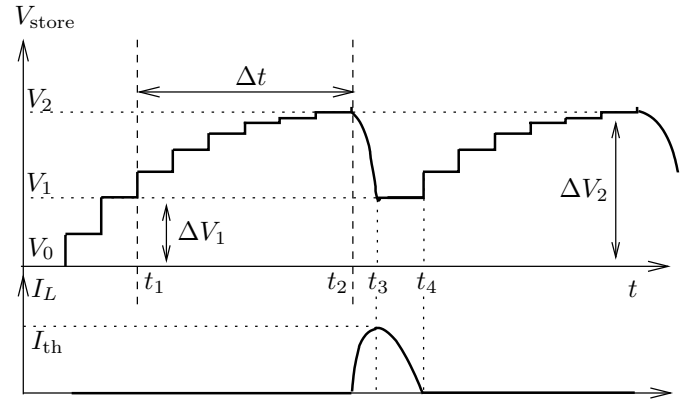


Figure 3: Time evolution of V_{store} and I_L during a complete cycle "charge pump - flyback circuit" (t_1-t_4). (t_1-t_2): charge pumping, (t_2-t_3): switch is ON, (t_3, t_4): switch is OFF, $D3$ is ON.

As the switch getting off, ΔV is the same as at some moment t_1 , and $\Delta V = \Delta V_1$, $I_L = I_{th}$, and C_{store} is cut from the network. ΔV_1 is a design parameter: $0 < \Delta V_1 < \Delta V_2$, and is actually defined by the time during which the switch is on. Following the principle of a BUCK DC-DC converter, when the switch becomes off, the current continues through $D3$ which becomes on. The new equivalent LC network is such that $C = C_{res}$. It starts with a non-zero V_C and I_L , and is polarized such that I_L charges C so that V_C increases. When I_L becomes zero, $D3$ cuts off, achieving the operating cycle of the flyback circuit.

Since at $t = t_3$ $V_C = V_{res}$ has the same value as at $t = t_1$, between t_3 and t_4 V_{res} becomes superior to $V_{res}(t_1)$. When I_L becomes zero, the diode $D3$ is cut off, and the circuit return to virtually the same state as before charge pumping, at $t = t_1$, but with a slightly higher V_{res} .

In this way, the energy gained by the pump and accumulated in the inductor (or a part of it, if $\Delta V_1 \neq 0$) is provided to C_{res} , i.e., the charges of the electrical ground are separated which increases the amount of non-compensated charges in the circuit. Thus, in theory, the

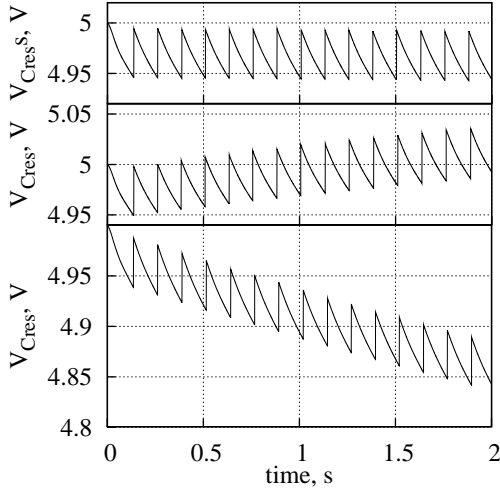


Figure 4: Evolution of V_{res} for different load resistance values. Data obtained by simulation of the circuit described in section 4.1. From top to down : $R=26 \text{ M}\Omega$, $R=30 \text{ M}\Omega$, $R=20 \text{ M}\Omega$.

mean value of V_{res} should increase slowly. In practice, the circuit is continuously losing charges : because of the load, of course, but also because of the parasitic leakage, so that at steady mode the additional charge put on C_{res} is exactly equal to the charge consumed by the load during the cycle "charge pump + flyback". Actually, the principle of the harvester operation is to renew the C_{res} charges consumed by the load. The plot fig. 4 presents the V_{res} voltage evolution for the cases when the load in adequation with the flux of electrical charges provided by the harvester (steady mode), when the load resistance is too high and too low.

In this way, in the equilibrium mode the charge pump starts always from ΔV_1 , operates until ΔV_2 , and the flyback phase reduces ΔV from ΔV_2 to ΔV_1 , making possible a cyclic operating of the system, as shown in the fig. 3.

The energy harvested during such a cycle can be calculated from the fig. 2, in function of the number of pump cycles. It is easy to understand that this is the energy available for the load, thus, it is possible to calculate the maximal load (minimal resistance) using the relation $\Delta W = V_{\text{res}}^2/R \cdot \Delta t$, Δt being the duration of charge pumping.

In the above analysis, we assumed for the simplicity that the diode forward voltage is zero. In the case $V_d \neq 0$ the minimal value for ΔV is not zero, but $2V_d$. Thus, the use of non-ideal diodes limits the choice for ΔV_1 imposing a non-zero low limit for this parameter.

3 Optimal switch operation

The commutation timing of the switch determines the efficiency of the energy harvesting. In previous papers,

an asynchronous commutation has been used, i.e., the switch commutated periodically with some fixed duty ratio [1]. However, this solution is not appropriate when the environment parameters, e.g. the vibration frequency, change. Indeed, in this case the V_{store} curve of the fig. 3 scales horizontally, and if the commutation timing is fixed, ΔV_1 and ΔV_2 can change, yielding a suboptimal harvester operation.

3.1 Optimal operation and time markers

The optimal Δt window for the charge pump operation is given by $t(V_1)$, $t(V_2)$ so that $\frac{W[t(V_2)] - W[t(V_1)]}{t(V_2) - t(V_1)}$ is maximum over $V_1, V_2 \in (V_0, V_{\text{sat}})$ (V_{sat} is the saturation voltage of the pump charge, $V_{\text{sat}} = V_0 C_{\text{max}}/C_{\text{min}}$). This maximum can be found numerically and a rather complex analytical expression can be provided. However, it comes from the plot in fig. 2 that $W(n)$ has three zones : small parabolic at low n , then large linear with the maximal slope, and then asymptotical, with decreasing slope. Thus, $t(V_2)$ should be chosen at the end of the linear zone, and $t(V_1)$ can be zero or be situated at the beginning of the linear zone. We made an analysis assuming that $t_1 = 0$, $V_1 = V_0$, and found an algebraic equation allowing a calculation of an optimal V_2 . Here we give a summary of this analysis.

For the simplicity, we assume that the presence of the load resistance doesn't modify the operation of the charge pump, i.e., $RC_{\text{res}} \gg \max(\Delta t)$. Thus, at the beginning of the pump operation, the energy of C_{res} and C_{store} is

$$W_0 = (C_{\text{res}} + C_{\text{store}})V_0^2/2. \quad (1)$$

At t_2 , when $V_{\text{store}} = V_2$, $V_{\text{res}2} = V_{\text{res}}(t_2)$ can be found from the charge conservation law :

$$Q_0 = (C_{\text{store}} + C_{\text{res}})V_0 = C_{\text{store}}V_2 + C_{\text{res}}V_{\text{res}2}. \quad (2)$$

At t_2 , the energy is given by :

$$W_2 = C_{\text{res}}V_{\text{res}2}^2/2 + C_{\text{store}}V_2^2/2. \quad (3)$$

From (1-3) we get the harvested energy :

$$\Delta W = C_{\text{store}}(1 + C_{\text{store}}/C_{\text{res}})(V_2 - V_{\text{res}2})^2/2. \quad (4)$$

However, what we are interested in is not the absolute energy, but the power. Thus, we will look for V_2 maximizing the following :

$$P = \Delta W/(n(V_2)T), \quad (5)$$

where $n(V_2)$ is the number of pump cycles needed to reach $V_{\text{store}} = V_2$ from $V_{\text{store}} = V_0$, and T is the period of vibrations.

From (8) of [1] we know that

$$n = \log \frac{C_{\text{store}}}{C_{\text{min}} + C_{\text{store}}} \frac{V_2/V_0 - C_{\text{max}}/C_{\text{min}}}{1 - C_{\text{max}}/C_{\text{min}}} \quad (6)$$

Introducing $\theta = V_2/V_0$ and supposing $V_{res} \approx V_0$, from the above formula we have for the power :

$$P = K \cdot \frac{(1 - \theta)^2}{\ln \frac{\theta - a}{1 - a}}, \quad (7)$$

where $a = C_{max}/C_{min}$ and K is a constant calculable from C_{max} , C_{min} , T and V_0 .

By looking for zero of the derivative, we conclude that $P(\theta)$ has a maximum given by the root of the equation:

$$2 \ln \frac{\theta - a}{1 - a} = (1 - a)(\theta - a). \quad (8)$$

The θ obtained by numerical resolution of this equation gives to the optimal threshold value of V_{store} at which the switch should become "ON". Thus, the "OFF-ON" commutation of the switch can be controlled by this voltage.

There are many possibilities to detect the moment when the switch should become "OFF". It should happen when the voltage difference $V_{store} - V_{res}$ becomes zero (or some low threshold value), or otherwise, when the switch current becomes maximal, i.e., a current threshold can be defined. The maximal current value can be deduced using the energy considerations :

$$\frac{C_{store}C_{res}}{C_{store} + C_{res}}(V_2 - V_0)^2 = LI_{max}^2. \quad (9)$$

3.2 Commutation of the switch

The above considerations demonstrate that the commutation should be ordered not by a timing scenario, but by the energy state of the circuit, i.e., the voltage and/or current levels. We proposed the following model for the switch.

$$\begin{cases} U = R_{on}I, & \text{if ON="1" and } I < I_{th} \\ ON = "0", & \text{if ON="0" and } I > I_{th} \\ U = R_{off}I, & \text{if ON="0" and } V_{control} < V_{th} \\ ON = "1", & \text{if ON="0" and } V_{control} > V_{th} \end{cases} \quad (10)$$

We give here a VHDL-AMS implementation of this mathematical model. Such a switch is an element with memory ("ON" is a boolean variable) recalling its current state.

```
entity three_poles_switch is
  GENERIC (von:emf:=0.7;
           ihold: current := 0.0;
           R_close : real:=1.0e-12;
           R_open  : real:=10.0e6;
           imax: real:=2.0);
  PORT ( TERMINAL ep: Electrical ;
         TERMINAL em: Electrical ;
         TERMINAL gate: Electrical);
END ENTITY thyristor_limiting_adms_vhdlams;
```

```
ARCHITECTURE vhdlams OF three_poles_switch IS
  quantity v across i through em to ep;
```

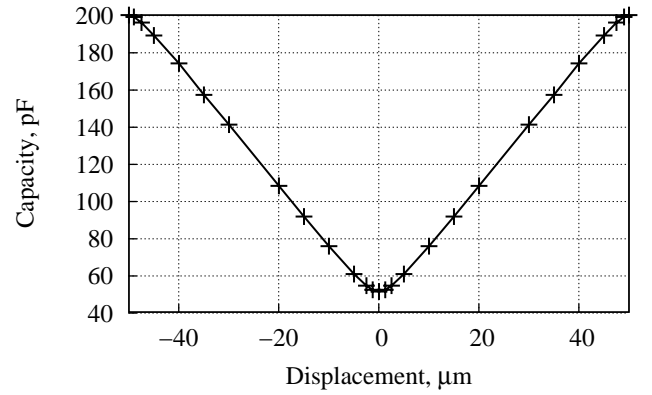


Figure 5: Evolution of C_{var} with the resonator position. Data obtained by 3D finite-element simulation.

```
quantity v_ctrl across em to gate;
signal ison : boolean;
PROCESS
  variable off: boolean := true;
BEGIN
  ison <= NOT off;
  CASE off IS
    WHEN true =>
      WAIT UNTIL v_ctrl 'above(von);
      off:=false;
    WHEN false =>
      WAIT UNTIL i 'above(imax);
      off:=true;
  END CASE;
END PROCESS;
IF ison USE iscr==vscr/R_close;
ELSE i = vscr/R_open;
END USE;
BREAK ON ison;
END ARCHITECTURE adms_vhdlams;
```

4 VHDL-AMS model of the electromechanical part

The prototype for the model of the resonator and electromechanical transducer was the device presented in [3]. This is a "mass-spring" system associated with a variable capacitor of comb geometry. The law of capacitance evolution over the electrode displacement x is given in fig. 5, and is fit by a piecewise-defined polynomial function (whose code is omitted in the listing given below).

The system is modeled as a block which takes one input value : the external vibration acceleration. The model takes into account the inertial properties of the mechanical resonator and $C(x)$ relation given in fig. 5. At the output, the model provides a capacitor whose capacitance varies according to the external vibrations and mechanical system dynamics.

The electromechanical resonator is also provided with stoppers limiting the displacement by $\pm 50 \mu\text{m}$ (the scope

of the plot in fig. 5). We modeled the stoppers as highly viscous walls (μ_v is the viscosity, v is the velocity) :

$$F_{\text{stopper}} = -\mu_s v, \text{ if } |x| > 50 \mu\text{m} \quad (11)$$

The modeling of the stoppers allows to study the cases where the transient amplitude of the mass vibration is superior to x_{max} , whereas the steady-state amplitude value is in the acceptable limits.

The other equations underlying the electromechanical model are given and commented in the model listing.

```
ENTITY harvesting_resonator_adms_vhdlams IS
  GENERIC (
    Q0:real:=5.53e-11); -- initial charge,
                                Q0=5v*11pF
  -- capacitance terminals
  PORT (terminal e1, e2 : electrical;
  -- input acceleration terminal
  -- defined as electrical so to be set as
  -- voltage in Analog Artist environnement
    terminal accel : electrical);
END;
```

```
ARCHITECTURE adms_vhdlams OF
  harvesting_resonator IS
  constant m: real:=46.0e-6; -- mass
  constant k: real:=152.6; -- stiffness
  -- resonator damping
  constant kv: real:=2.185e-3;
  -- stopper damping
  constant mu_stopper: real:=100.0;
  -- stopper position
  constant xmax: real:=50.0e-6;
  -- permittivity of vacuum
  constant epsilon: real:=8.85e-12;
  -- Capacitance voltage and current
  quantity vC across iC through e1 to e2;
  -- quantity for the input acceleration
  quantity a_ext across accel
    to electrical_ground;
  -- displacement
  quantity x: real:=0.0;
  -- velocity
  quantity velocity : real:=0.0;
  -- electrical charge
  quantity charge : real:=0.0;
  -- Variable capacitance
  quantity Cvar : real;
  -- Electrical force
  quantity Felec : real;
  -- resonator accel.
  quantity acceleration : real;
  -- dCvar/dX
  quantity dCvar_dx : real;
  -- stopper force
  quantity Fstopper : real;
```

```
BEGIN
  -- a=v'=x''
  velocity==x'dot;
  acceleration==velocity'dot;
  -- Capacitance and its derivative
```

```
Cvar==cap_ESYCOM(x);
dCvar_dx==dcap_dx_ESYCOM(x);
-- Capacitance charge
charge==Cvar*vC+Q0;
-- electric force
Felec==vC*vC*dCvar_dx/2.0;
-- stopper force calculation
if (abs(x)>xmax) use
  Fstoppers==vitesse*mu_stopper;
else Fstoppers==0.0;
end use;
-- second law of Newton
m*acceleration==k*x-kv*vitesse
+Felec-m*a_ext+Fstoppers;
-- el. current calculation
iC==charge'dot;
end adms_vhdlams;
```

4.1 Harvester model

The actual model of the harvester includes the variable capacitor VHDL-AMS model, the above presented switch model and the ELDO models of the other components in fig. 1 circuit. For the diodes, ideal models with $V_d = 0$ were used.

The whole system was simulated in CADENCE Analog Artist environment with ADVanceMS simulator of Mentor Graphics. The schematic view of the circuit is presented in the fig. 6.

5 Simulation results and conclusions

Fig. 7 presents the simulation results of the circuit in the fig. 6 : the upper plot provides a global view of the circuit state evolution law, the lower plots offer an insight in the pump charge and flyback network operation.

With external acceleration magnitude of 10 m/s² and frequency of 298 Hz, we observed a C_{var} variation between 174 pF and 51.6 pF. With these values, the presented above theoretical considerations give for the switch "OFF-to-ON" commutation $n = 80$, which corresponds to $V_{\text{store}} = 13.4V$. This correspond to $I_L = 9.7$ mA for the switch "ON-to-OFF" commutation moment. The theoretical minimal load resistor is 32 M Ω .

The plot in fig. 4 presents the evolutions of V_{res} for different R_{load} . We can see that the real minimal resistance is somewhat lower. This is explained by the fact that the switch becomes "OFF" before $I_L = 0$ and $V_{\text{store}} = V_{\text{res}}$: it can be seen on the $V_{\text{store}}(t)$ graph (the upper plot in fig. 7) that V_{store} does not reach V_0 , i.e., $V_1 > V_0$. As it can be seen from the the plot of $W(n)$ of fig. 2, the low-slope starting zone of $W(n)$ is avoided, and the harvester operates on the maximal slope zone of $W(n)$ yielding a bit higher energy efficiency. From $W(n)$ the maximal harvested power (thus the minimal load resistance) can be

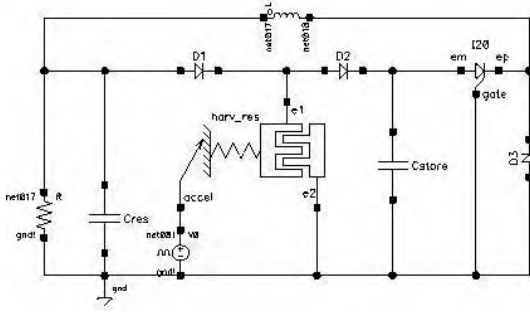


Figure 6: Schematic view of the complete harvester model. The VHDL-AMS models of the devices *harv_res* and *I20* are given below. $L = 2.5$ mH, $C_{res} = 1$ μ F, $C_{store} = 3.3$ nF.

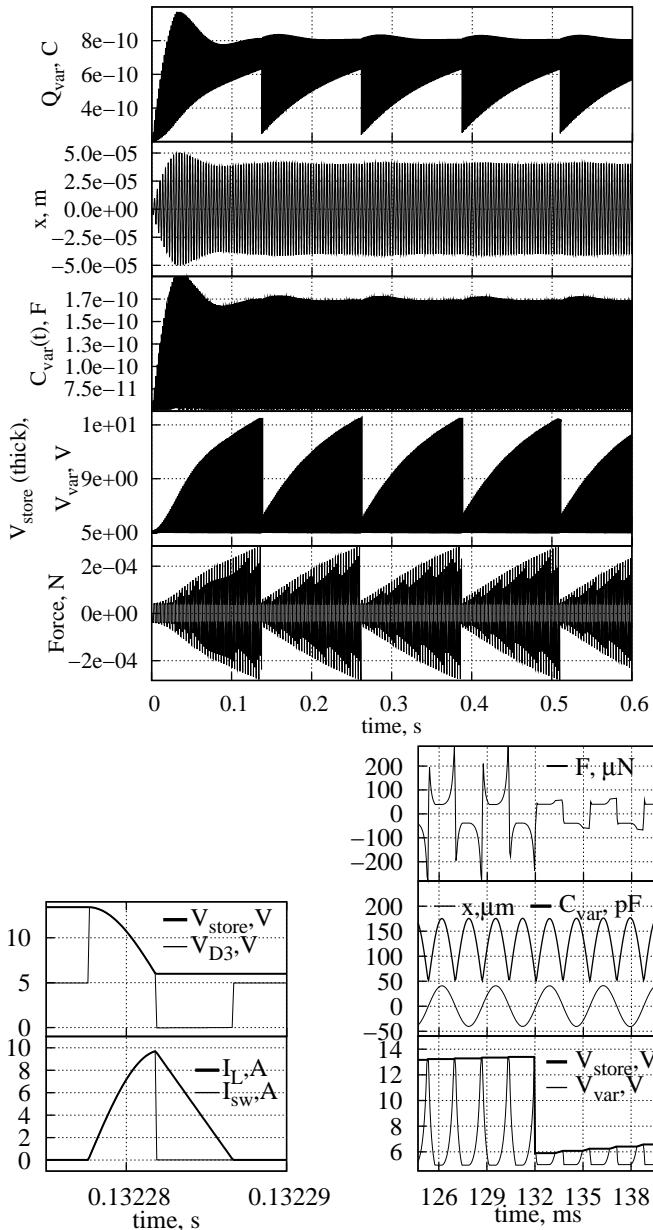


Figure 7: Simulation results of the harvester mixed model (fig. 6)

calculated : we obtained 26 M Ω , i.e., slightly lower than the value given by the above presented analysis.

We also observed a phenomenon related to the electromechanical coupling. The displacement magnitude, and thus the C_{var} variation magnitude, does depends not only on the external acceleration (which is constant), but also on the state of the conditioning circuit. From the upper plot in fig. 7 giving the C_{var} evolution envelope, one can see that after each flyback phase the capacitance and displacement (x) amplitudes increase slightly, whereas the voltage amplitude on C_{var} decreases from V_2 to V_1 . In fact, this is an effect of non-linearity of the capacitive transducer : when biased, it behaves like an electrostatic spring [4] whose stiffness depends on the voltage: thus, the resonator resonance frequency is not exactly the same at the beginning and at the end of the charge pumping, which results a vibration amplitude variation.

6 Conclusions

The control of the switch commutation by the internal state of the circuit is a very interesting concept, which needs reliable analytical and modeling tools to be explored. The proposed technique of commutation control is not the only possible: one can imagine to control the "ON"- "OFF" commutation by sensing the voltage $V_{store} - V_{res}$ and by detecting when it crosses zero or some other value.

In perspective, it is necessary to get a deeper insight in the optimal conditions of the energy harvester operations, and to address issues such as parasitic phenomena.

References

- [1] B. C. Yen and J. H. Lang, "A variable-capacitance vibration-to-electric energy harvester," *IEEE transaction on Circuits and Systems - I: Regular Papers*, vol. 53, pp. 288–295, february 2006.
- [2] C. H. Haas and M. Kraft, "Modeling and analysis of a mems approach to dc voltage step-up conversion," *Journal of Micromechanics and Microengineering*, vol. 14, pp. s114–s122, 2004.
- [3] A. M. Paracha, P. Basset, P. Lim, F. Marty, and T. Bourouina, "A bulk silicon-based vibration-to-electric energy converter using an in-plane overlap plate (ipop) mechanism," *Proc. of PowerMEMS2006*, pp. 169–172, 2006.
- [4] D. Galayko, A. Kaiser, B. Legrand, L. Buchailot, D. Collard, and C. Combi, "Coupled-resonator micromechanical filters with voltage tunable bandpass characteristic in thick-film polysilicon technology," *Sensors and Actuators A: Physical*, vol. 126, pp. 227–240, january 2006.